

# On the possibility of generating low-energy positrons on accelerators of electrons with a beam energy of a few MeV and on terawatt lasers

D.A. Gorlova, V.G. Nedorezov, K.A. Ivanov, A.B. Savel'ev, A.A. Turinge, I.N. Tsymbalov

**Abstract.** Based on the numerical simulations, we estimate the possibility of generating positrons by low-energy electrons (below 10 MeV) produced by electron accelerators and femtosecond lasers. A review of experimental work reported in the literature is presented. The simulation is carried out using the GEANT-4 software package for the particular conditions of a possible experiment at the terawatt femtosecond laser facility of the International Laser Centre at the Moscow State University and the LUE-8 MeV linear electron accelerator at the Institute for Nuclear Research, Russian Academy of Sciences.

**Keywords:** positrons, accelerators of electrons, femtosecond lasers.

## 1. Introduction

The investigation of generation of low-energy (up to 10 MeV) positrons has actively developed in recent years, including the techniques using femtosecond lasers (see, e.g., review [1]). The reason is that these studies are important for the solution of fundamental and applied problems. Thus, at CERN, the investigation devoted to the dark matter search and the processes beyond the Standard Model are in progress [2]. An important applied method is the annihilation spectroscopy that allows a structure of different materials to be studied, including metals, polymers, ceramics, composites, etc. [3], at a microscopic level.

The major amount of work in this field is presently implemented on accelerators of electrons. Among the latter, worth noting is the linear accelerator at the Argonne Laboratory (USA) with an electron energy of 15 MeV and a beam current of 200  $\mu\text{A}$ , the AIST linear accelerator (7–70 MeV, 100  $\mu\text{A}$ ) in Tsukuba (Japan), the NAMI microtron (170 MeV, 75  $\mu\text{A}$ ) in Mainz (Germany). These accelerators allow the generation of positron beams with the flux up to  $10^8$  positrons per sec-

ond. Such a flux is achieved using the technologies, related to porous thin-film targets and magnetic traps [4].

In a wide class of problems an alternative to the above accelerators of electrons are the laser plasma accelerators of electrons [5, 6], based on the excitation of a so-called plasma wakefield. To date, the experimental techniques are found and experimentally approved, providing the formation of the electron pulse with a mean electron energy up to a few GeV, a spectral width equal to parts of percent of the energy value, a charge up to 1 nC, and a beam divergence of a few mrad. However, the low repetition rate of the laser and, therefore, the electron pulses (certainly lower than 10 Hz) provides no possibility of obtaining a high mean beam current, which makes photonuclear studies difficult. It is interesting to compare different methods in order to implement their positive features.

The main specific feature of laser methods is a very small pulse duration and a gamma spectrum envelope sharply falling with increasing energy. This allows one to measure the probability (cross section) of photonuclear processes having threshold behaviour within a relatively narrow energy range of the incident gamma quanta and refer such pulses of gamma quanta to as monochromatic ones.

Positrons can be generated also in the process of direct interaction of a high-power relativistic laser pulse with a dense target, leading to the acceleration of electrons deep into the target. In this case, the energy of the electrons appears to be essentially lower, but their number is significantly higher. Further interaction of such electrons with the same target leads (if the energy of electrons is sufficient) to the production of electron–positron pairs.

Note that in the long term at a laser intensity above  $10^{28} \text{ W cm}^{-2}$ , which is by six orders of magnitude higher than the up-to-date intensities at top-class facilities, it will be possible to consider the electron–positron pair production due to the vacuum polarisation [7]. The situations are being theoretically considered, in which this threshold can be essentially lowered at the expense of quantum electrodynamic cascades [8], special field geometry [9], etc. The experimental observation of this effect is hardly probable in the nearest future.

In the present paper the schemes of optimal experiments on generating low-energy positrons using the terawatt femtosecond laser facility of the International Laser Centre, Moscow State University, (ILC MSU) and the LUE-8 MeV electron accelerator at the Institute for Nuclear Research of the Russian Academy (INR RAS) are developed based on the numerical simulation. A review of papers devoted to the positron production by means of femtosecond lasers and accelerators at energies below 10 MeV is presented.

**D.A. Gorlova, K.A. Ivanov, A.B. Savel'ev** Faculty of Physics and International Laser Centre, M.V. Lomonosov Moscow State University, Vorob'evy Gory, 119991 Moscow, Russia;

e-mail: gorlova.da14@physics.msu.ru, abst@physics.msu.ru;

**I.N. Tsymbalov** Faculty of Physics and International Laser Centre, M.V. Lomonosov Moscow State University, Vorob'evy Gory, 119991 Moscow, Russia; Institute for Nuclear Research, Russian Academy of Sciences, prosp. 60-letiya Oktyabrya 7a, 117312 Moscow, Russia;

**V.G. Nedorezov, A.A. Turinge** Institute for Nuclear Research, Russian Academy of Sciences, prosp. 60-letiya Oktyabrya 7a, 117312 Moscow, Russia; e-mail: vladimir@cpc.inr.ac.ru

Received 19 February 2017; revision received 16 March 2017

*Kvantovaya Elektronika* 47 (6) 522–527 (2017)

Translated by V.L. Derbov

## 2. State of the art

At present two main processes are specified that lead to the electron–positron pair production in the interaction of relativistic electrons with a nucleus, namely, the Trident process (TP) [10] and the Bethe–Heitler process (BHP) [11]. The first of them is the scattering of an electron by the Coulomb field of a nucleus having a charge  $Z$ :

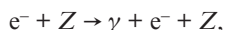


The total differential cross section of the TP can be described by the formula

$$\sigma_{e^- \rightarrow 2e^+} = 5.22Z^2 \ln^3 \left[ \frac{2.30 + E_a}{3.52} \right],$$

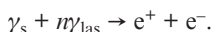
where  $E_a$  is the energy of the electron (MeV) (the cross section being expressed in microbarns).

The Bethe–Heitler process occurs in two stages. At the first stage, the electron interacting with the nucleus emits a high-energy bremsstrahlung photon  $\gamma$ . At the second stage, this photon produces an electron–positron pair in the Coulomb field of the nucleus:



Both processes strongly depend on the charge  $Z$  of the nucleus, so that for efficient generation one should use heavy nuclei as targets.

At high laser radiation intensities, the multiphoton Breit–Wheeler effect is sometimes considered, in which the pair is produced due to the interaction of a bremsstrahlung photon  $\gamma_s$  with  $n$  photons of laser radiation  $\gamma_{\text{las}}$ :



Note for generality that the pair production is also possible as a result of the  $e^-e^-$  and  $e^-\gamma$  interaction. However, the cross section of these processes is small and, therefore, their effect is insignificant. In the present paper, only TP and BHP will be considered.

The published results obtained on accelerators at energies below 10 MeV are few. Figure 1 presents the dependences of the coefficient of  $e^-e^+$  conversion on a tantalum target (as thick as nearly one radiation length) on the energy of positrons. The analysis of the data presented in Fig. 1 shows that they considerably differ among themselves and, as shown below, from the results of numerical simulation. Therefore, keeping in mind the present-day great interest to the construction of positron sources, one can conclude that new experimental data are required.

As mentioned above, in the case of using intense laser pulse, two main schemes are applied to produce electrons with the energy required for subsequent positron generation. In the single-stage scheme, the electrons are produced in the process of interaction of laser radiation with a dense target, in which the positrons are generated. In the double-stage scheme, the beam of electrons is obtained by their acceleration in the plasma wave, excited in relatively rarified plasma, and then this beam is incident on a special target to produce positrons (Fig. 2). Let us consider these schemes in more detail.

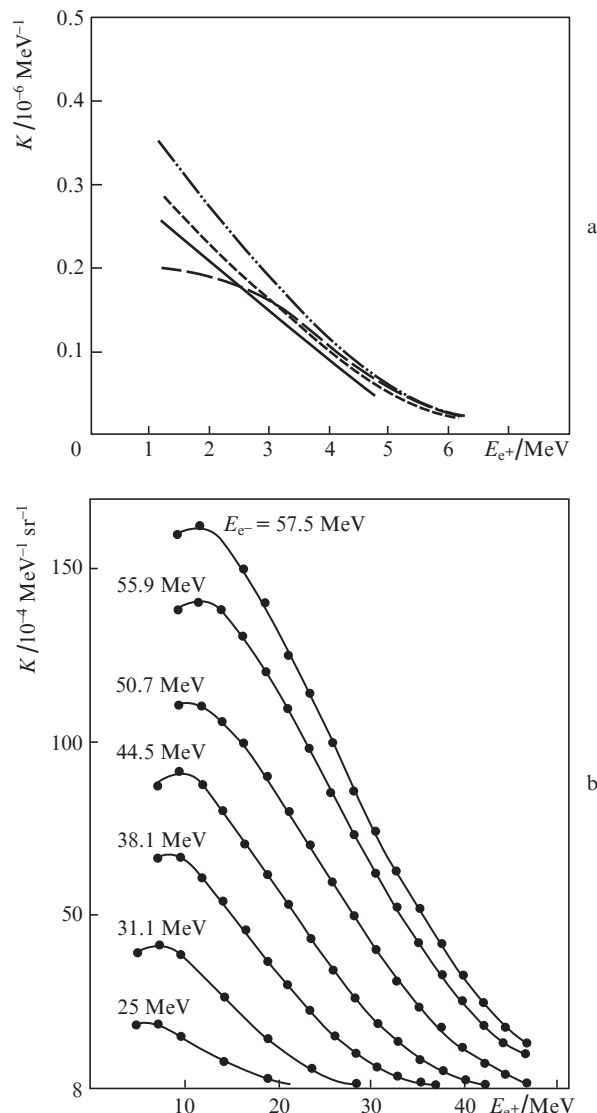


**Figure 1.** Dependence of the  $e^-e^+$  conversion coefficient  $K$  for the tantalum target on the energy of positrons  $E_{e^+}$  in the solid angle  $5 \times 10^{-3} \text{ sr}$  for the energy of electrons  $E_{e^-} = 9.3 \text{ MeV}$ , the target thickness  $0.5\text{--}2 \text{ mm}$  [12] (a) and in the complete solid angle for different electron energies [13] (b).

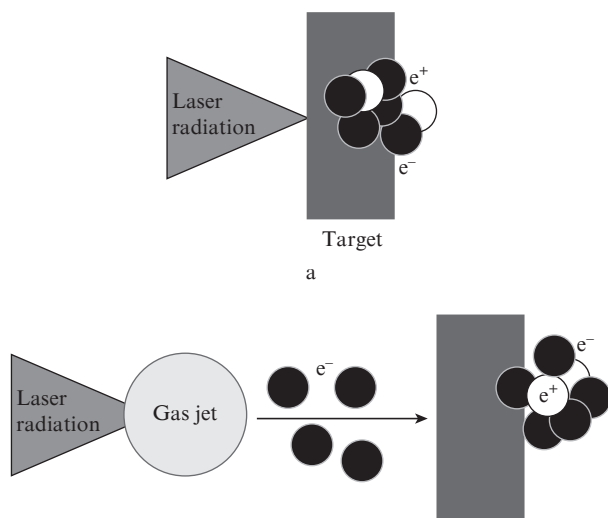
The results of the experimental studies [14–22] of positron production by means of lasers are presented in Table 1. The first study of the single-stage scheme was performed in 2009 [14]. The measurement of positron and electron spectra for different materials allowed experimental demonstration of the dependence of the cross section of positron production on the nuclear charge  $Z$  of the target. For the first time the anisotropy of the angular spectrum of positrons was experimentally detected, namely, the emission from the front surface of the target appeared to be nearly by 10 times greater than from the side surface.

In Ref. [15] the angular spectrum of positrons and the dependence of the obtained energies on the target thickness were thoroughly studied. It was shown that the positrons are generated in the form of a quasi-monochromatic beam with a divergence of  $\sim 20^\circ$  (FWHM), which corresponds to the angular divergence of the formed electron beam. With increasing pulse energy, the mean energy of the generated positrons also increases and the divergence of the positron beam decreases.

**Table 1.** Review of experimental schemes of positron production.

Facility	Parameters	Range of detected positron energies/MeV	Material, shape, and geometric parameters of the target	Number of positrons per pulse	Reference
Titan laser, Jupiter laser (LLNL)	$\lambda = 1054$ nm $\tau = 0.7\text{--}10$ ps $E_{\text{las}} = 120\text{--}250$ J	0.1–100	Au, Ta, Sn, Cu, Al, disks, $d = 6.4$ mm, $h = 0.1\text{--}3.1$ mm	$10^9$	[14]
Titan laser (LLNL), OMEGA EP	$\lambda = 1054$ nm $\tau = 10$ ps $E_{\text{las}} = 100\text{--}850$ J $I = 10^{19}\text{--}5 \times 10^{20}$ W cm $^{-2}$	0.1–100	Au, disks, $d = 1\text{--}20$ mm, $h = 1$ mm	$10^{10}\text{--}10^{12}$	[15, 16]
Texas Petawatt laser	$\lambda = 1057$ nm $\tau = 130\text{--}245$ fs $E_{\text{las}} = 80\text{--}130$ J $I = 10^{21}$ W cm $^{-2}$	1–130	Au, Pt, disks, $d = 2\text{--}4.5$ mm, $h = 0.1\text{--}6$ mm; rods, $d = 2\text{--}3$ mm, $l = 4\text{--}10$ mm	$10^{10}$	[17]
MPQ (ATLAS laser)	$\lambda = 790$ nm $\tau = 130$ fs $E_{\text{las}} = 220$ mJ $I = (4\text{--}6.5) \times 10^{18}$ W cm $^{-2}$	2	Gas – He, target – Pb, $h = 2$ mm	$10^6$	[18, 19]
HERCULES laser	$\lambda = 800$ nm $\tau = 30$ fs $E_{\text{las}} = 0.8$ J $I = 6 \times 10^{18}$ W cm $^{-2}$	80–250	Gas – 97.5% He, 2.5% N $_2$ , targets – Cu, Sn, Ta, Pb, $h = 1.4\text{--}6.4$ mm	$10^5$	[20]
Callisto laser (LLNL)	$\lambda = 800$ nm $\tau = 60$ ps $E_{\text{las}} = 6.5$ or 10 J	0–350	Gas – He, target – Ta, $h = 1.5, 3$ mm	–	[21]
ASTRA-GEMINI	$\lambda = 800$ nm $\tau = 38\text{--}46$ fs $E_{\text{las}} = 14$ J $I = 3 \times 10^{19}$ W cm $^{-2}$	120–1200	Gas – He c 3.5% N $_2$ , target – Pb, $h = 0.5\text{--}4$ cm	$10^8$	[22]
Shanghai Institute of Optics and Fine Mechanics	$\lambda = 800$ nm $\lambda = 45$ fs $E_{\text{las}} = 3.75$ J $I = 3.5 \times 10^{19}$ W cm $^{-2}$	0–50	Gas – Ar, target – Pb, Cu, $h = 2$ mm	$10^6$	[23]
Stanford Linear Collider	Electron beam: 120 Hz, 30 GeV, 30 kW. The accelerator length is 2 km.	2–20	W(90%)–Rh(10%)–target, $h = 24$ mm	$10^{10}$	[24]

Note:  $d$ ,  $h$  and  $l$  are the diameter, thickness and length of the target;  $\lambda$ ,  $\tau$ ,  $E_{\text{las}}$  and  $I$  are the radiation wavelength, pulse duration, energy and intensity of the laser pulse, respectively.

**Figure 2.** (a) Single-stage and (b) double-stage schemes of positron generation.

The increase in the target diameter is accompanied by the fall of the mean energy of the positrons. The optimisation of the experimental configuration allowed an essential increase in the number of positrons produced by a single laser pulse [16].

Note that in this method of positron beam generation the beam divergence appeared smaller by nearly two times than the values, typical for the beams obtained at linear accelerators (see Table 1). However, the present data are insufficient for final conclusions.

In Ref. [17], the spectra of positrons for different shapes of the target were analysed. It was found that the positron yield significantly increases in the targets having the shape of rods, since in this case the thickness of the target is sufficient for efficient pair production and the losses due to the emission of positrons in the radial direction are minimal at the expense of the small rod diameter. At the same time, the maximal density of electron–positron pairs is achieved using thick targets having the shape of a disc.

The pioneering experiments on the positron generation using the double-stage scheme were implemented at the very beginning of the XXI century [18, 19]. In these studies, the positron detection threshold amounted to  $\sim 2$  MeV, the posi-

tron yield being about 25 positrons per pulse. Such a small number of the observed positrons led to the fact that the next experiments using this scheme were undertaken only 10 years later [20].

In these experiments, in agreement with the theory, the maximal positron energy and yield were observed in the targets with a higher  $Z$ . The dominant mechanism was the BHP, for which the number of positrons is proportional to the square of the target thickness  $h$ . Good agreement with this dependence was obtained in Pb and Ta targets. While in the earlier experiments not enough attention was paid to the optimisation of electron acceleration in the gas jet, in the recent paper [21] the study of double-stage positron generation using the electrons accelerated in the wakefield was presented. However, at the parameters of the setup, similar to those of Ref. [22], no positron signal was detected, which might be due to the high detection threshold.

Further optimisation of the experimental scheme [23] from the point of view of improving the parameters of the electron beam (the maximal energy 600 MeV, the angular divergence 2 mrad (FWHM), the flux  $\sim 10^9$  electrons per second) allowed essential improvement of the resulting positron yield. The maximal energy of the positrons was achieved at the converter target thickness of 0.5 cm, which is nearly equal to the radiation length of electrons for Pb, and the maximal yield was observed at the thickness of 1 cm. At the target thickness  $\sim 2.5$  cm, the electron–positron plasma became neutral with the total number of particles of each sort,  $3 \times 10^7$ , and the beam divergence 5–20 mrad. Similar results were obtained in Ref. [24]. The produced beam of electrons with the energy 50 MeV and the total charge 1.23 nC produced the positrons with the energy up to 42 MeV and the total number  $9.2 \times 10^6$ .

Thus, one can observe rapid progress in the positron beam generation using high-power laser pulses during the recent time. Two parallel approaches to the problem yield interesting and promising results. The scheme with direct irradiation of heavy targets at present provides a higher number of positrons per laser pulse; however, in this case the consumed energy of the laser pulse is essentially higher, too. Besides that, the best results are obtained using relatively long subpicosecond laser pulses. It is worth noting that in this case the positron beam divergence is rather large, although it appears to be smaller than that in the case of using linear accelerators of electrons. A much smaller divergence of the positron beam can be obtained using the second scheme with separate stages of laser-plasma acceleration of electrons and the production of positrons. In essence, this scheme is analogous to that applied in linear accelerators; however, the possibility to place the converter target very closely to the region of electron acceleration provides a small size of electron beam and allows the positron beam collimation to be achieved. We should note that to date the results on the production of positrons using both accelerators and high-power lasers are far from completeness and strongly differ. Therefore, new experimental and numerical studies are required to design positron sources with optimal parameters.

All considered schemes of positron production yield the particles with a rather high energy of a few tens or hundreds of MeV. At the same time, for applications the positrons of significantly lower energies are interesting. In this context, an important problem is also the production of electron–positron pairs near the reaction threshold, i.e., when the energy of electrons and gamma-quanta slightly exceeds  $2m_e c^2$ . To obtain such electrons, it seems reasonable to use compact electron

accelerators providing energies below 10 MeV and ‘tabletop’ femtosecond lasers with a peak power of a few terawatts. Moreover, these facilities are the ones that can find wide application due to their compactness and relatively low cost.

### 3. Simulation results and substantiation of planned experiments

To simulate numerically the process of positron generation by an electron beam, we exploited the widely used GEANT-4 software package [25]. The initial beam parameters were specified based on our previous experimental measurements of the spectra of electrons and gamma-radiation from the laser plasma at high contrast of the laser pulse [26–28], or corresponding to the parameters of the electron beam from the LUE-8 accelerator [29].

Figures 3 and 4 show the spectra and the angular distributions of positrons, normalised to the solid angle, at the exit from a 0.8 mm thick tantalum target, calculated using the GEANT-4 programme for three values of the initial energy of electrons. For the total number of electrons  $10^7$ , the yield of positrons at the initial energy of electrons  $E_{e^-} = 5, 7.5,$  and 19 MeV amounted to 2838, 13744, and 28906, respectively. Thus, the coefficient of  $E_{e^-}$  conversion has the order of

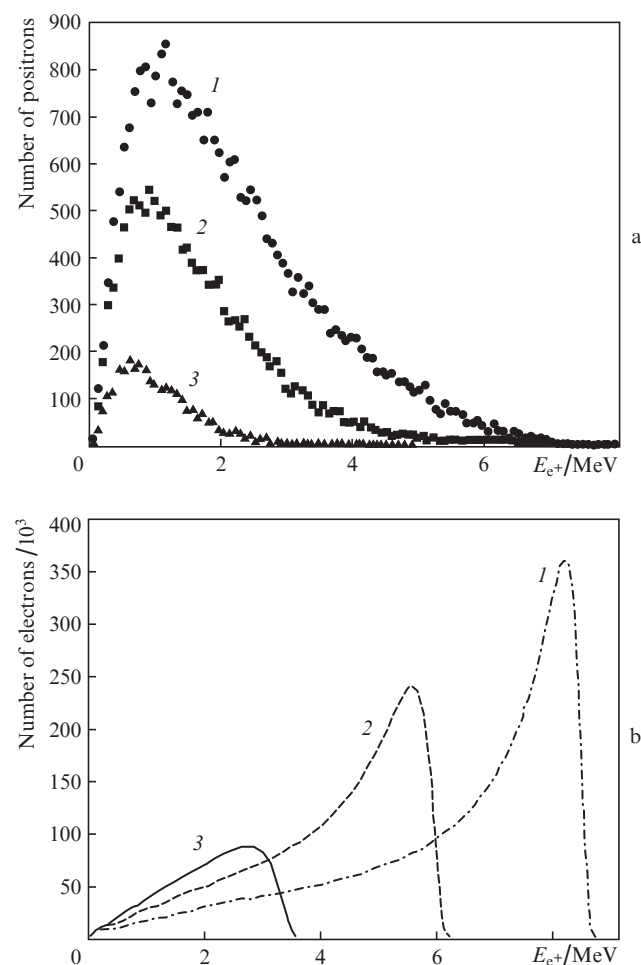


**Figure 3.** Energy distributions of (a) positrons and (b) electrons from a 0.8-mm-thick tungsten target. The energy of the incident electrons  $E_{e^-} = (1)$  10, (2) 7.5, and (3) 5 MeV.

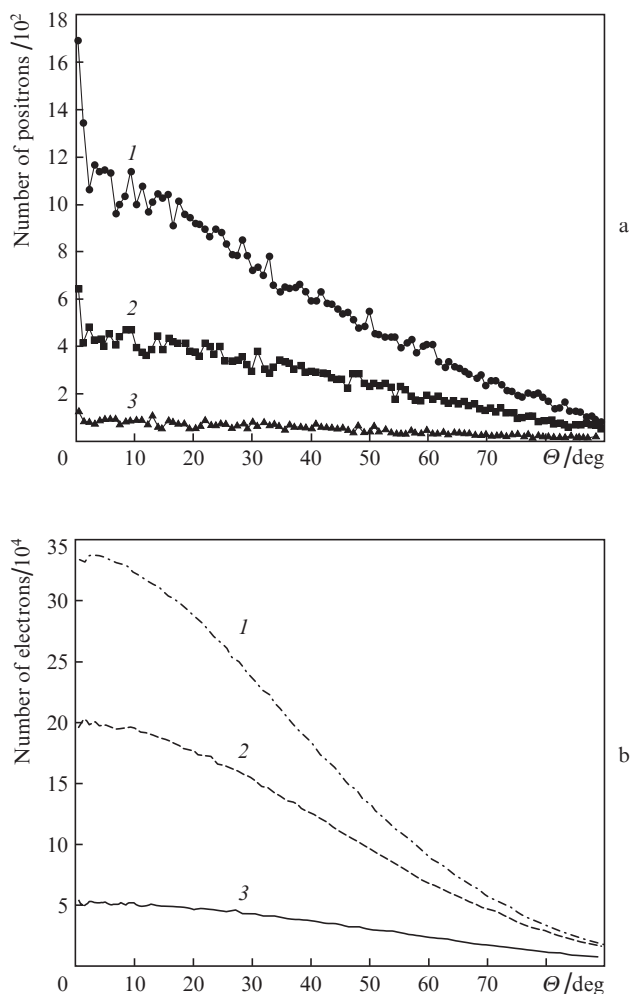


**Figure 4.** Angular distributions of (a) positrons and (b) electrons from a 0.8-mm-thick tungsten target. The energy of the incident electrons  $E_{e^-} = (1) 10$ , (2) 7.5, and (3) 5 MeV.

$10^{-4}$ – $10^{-3}$ , which allows one to expect a sufficiently high ( $\sim 10^4 \text{ s}^{-1}$ ) yield of positrons from the ILC MSU facility. In this case, the calculation of the positron production process using the accelerator beam yields the positron flux higher by six orders of magnitude.

In the same figures, the spectra and the angular distributions are presented for the electrons, passed through the radiator. It is seen that the electrons have a higher energy than the positrons. In contrast to the positrons, the upper boundary of the spectrum for the electrons is close to the initial energy of the beam. The energy of the positrons  $E_{e^+}$ , corresponding to their maximal yield, weakly depends on the energy of the electrons  $E_{e^-}$  and amounts to approximately 1 MeV. The maximal number of both positrons and electrons is observed in the direction of the initial electron beam propagation. For the positrons, a sharp maximum is observed in this direction, the relative amplitude of which rapidly grows with the energy of the primary electrons. At the same time, in the direction making an angle of  $10^\circ$  with this direction the number of positrons is only by two times smaller than in the direction along the axis.

The performed analysis has made it possible to propose the following scheme of a setup for studying the positron generation (Fig. 5). The key element of the setup is the magnetic

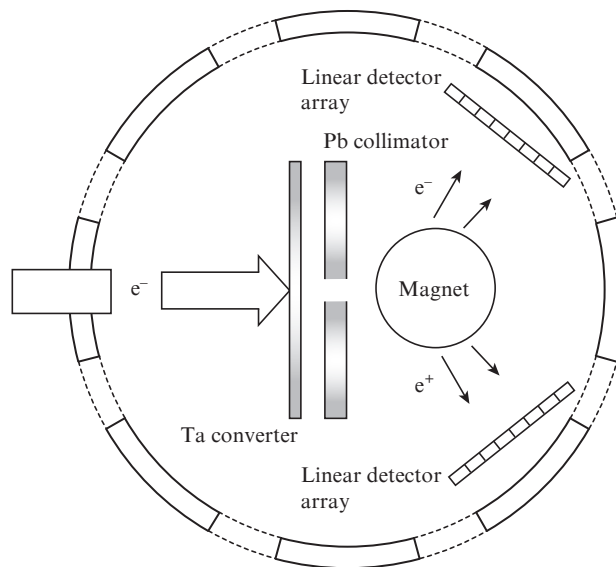


**Figure 5.** Schematic diagram of the proposed experiment.

spectrometer, described in detail in Ref. [30]. The beam of electrons with an energy from 1 to 8 MeV and a broad energy spectrum (up to 1 MeV) is incident on a tantalum converter plate having a thickness of 0.8 mm (the optimal thickness determined by means of simulation using the GEANT software package). The electron beam diameter amounts to  $\sim 0.8$  cm. The produced positrons and part of electrons pass through a 1-cm-thick lead collimator and enter the permanent magnet with a diameter of 5 cm and a magnetic field of 0.3 T. At the exit from the magnet, ten-channel scintillation linear arrays, operating in a single-electron (current) mode, are installed. The shield protecting the detectors against background radiation is not shown in Fig. 5. Note that the requirements to the spectrometer resolution are minimal ( $\sim 1$  MeV). The main goal is to measure the coefficient of conversion  $e^- \rightarrow e^+$  in the range of electron energies 1–8 MeV. The experiments are thought to be implemented independently on two facilities, the LYE-8 at INR RAS and femtosecond laser facility at ILC MSU. This will allow the improvement of the measurement accuracy and the assessment of the laser capabilities to serve as a source of low-energy positrons.

## 4. Conclusions

The numerical simulation of the positron generation process and the analysis of the available literature data for the energy range below 10 MeV show that the positron source can be based both on the linear accelerator LUE-8 at INR RAS and on the femtosecond laser facility at ILC MSU. The flux of low-energy (up to a few MeV) positrons can achieve  $10^{10} \text{ s}^{-1}$  at the accelerator and from  $10^4$  to  $10^6 \text{ s}^{-1}$  at the laser facility depending on the mode of laser pulse interaction with the target. Note that only such facilities can provide mass application of the developed approaches in different fields of research and engineering. The discussion of these issues is beyond the scope of the present paper and is a subject of multiple popular reviews available in the literature.

**Acknowledgements.** The work was supported by the Russian Foundation for Basic Research (Grant No. 16-02-00213).



## References

1. Habs D. et al. *AIP Conf. Proc.*, **1462**, 177 (2016).
2. Badertschier A. et al. *Phys. Rev. D*, **75**, 032004 (2007).
3. Grafutin V.I., Prokop'ev E.P. *Phys. Usp.*, **45** (1), 59 (2002) [*Usp. Fiz. Nauk*, **172** (1), 1 (2002)].
4. Chen H.M., Jean Y.C., Jonah C.D., Chemerisov S., Wagner A.F., Schrader D.M., Hunt A.W. *Appl. Surf. Sci.*, **252**, 3159 (2006).
5. Ledingham K.W.D., Spencer I., McCanny T., Singhal R.P., Santala M.I.K., Clark E., Watts I., Beg F.N., Zepf M., Krushelnick K., Tatarakis M., Dangor A.E., Norreys P.A., Allott R., Neely D., Clark R.J., Machacek A.C., Wark J.S., Cresswell A.J., Sanderson D.C.W., Magill J. *Phys. Rev. Lett.*, **84**, 899 (2000).
6. Malka G., Miquel J.L. *Phys. Rev. Lett.*, **77**, 75 (1996).
7. Narozhny N.B., Bulanov S.S., Mur V.D., Popov V.S. *JETP Lett.*, **80** (6), 382 (2004) [*Pis'ma Zh. Eksp. Teor. Fiz.*, **80**, 434 (2004)].
8. Mironov A.A., Fedotov A.M., Narozhny N.V. *Quantum Electron.*, **46**, 305 (2016) [*Kvantovaya elektronika*, **46**, 305 (2016)].
9. Bulanov S.S., Mur V.D., Narozhny N.B., Nees J., Popov V.S. *Phys. Rev. Lett.*, **104**, 220404 (2010).
10. King B., Ruhl H. *Phys. Rev. D*, **88**, 013005 (2013).
11. Bethe H. *Phys. Rev.*, **89**, 1245 (1953).
12. Bernardiny M. et al. *Saclay Report*, CEA, 2212 (1962).
13. Dzhilavyan L.Z., Lelekov A.V. *Kratkiye soobshcheniya po fizike Fizicheskogo Instituta Akademii Nauk SSSR*, (8), **37** (1979).
14. Chen Hui., Wilks S.C., Bonlie J.D., Chen S.N., Cone K.V., Elberson L.N., Gregori G., Meyerhofer D.D., Myatt J., Price D.F., Schneider M.B., Shepherd R., Stafford D.C., Tommasini R., Van Maren R., Beiersdorfer P. *Phys. Plasmas*, **16**, 122702 (2009).
15. Chen Hui, Wilks S.C., Meyerhofer D.D., Bonlie J.D., Chen C.D., Chen S.N., Courtois C., Elberson L., Gregori G., Kruer W., Landoas O., Mithen J., Myatt J., Murphy C.D., Nilson P., Price D., Schneider M., Shepherd R., Stoeckl C., Tabak M., Tommasini R., Beiersdorfer P. *Phys. Rev. Lett.*, **105**, 015003 (2010).
16. Chen Hui, Sheppard J.C., Meyerhofer D.D., Hazi A., Link A., Anderson S., Baldis H.A., Fedosejev R., Gronberg J., Izumi N., Kerr S., Marley E., Park J., Tommasini R., Wilks S., Williams G.J. *Phys. Plasmas*, **20**, 013111 (2013).
17. Liang E., Clarke T., Henderson A., Fu W., Lo W., Taylor D., Chaguine P., Zhou S., Hua Y., Cen X., Wang X., Kao J., Hasson H., Dyer G., Serratto K., Riley N., Donovan M., Ditmire T. *Sci. Rep.*, **5**, 13968 (2015).
18. Gahn C., Tsakiris G.D., Pretzler G., Witte K.J., Thirof P., Habs D., Delfin C., Wahlström C.-G. *Phys. Plasmas*, **9**, 987 (2002).
19. Gahn C., Tsakiris G.D., Pretzler G., Witte K.J., Delfin C., Wahlström C.-G., Habs D. *Appl. Phys. Lett.*, **77**, 2662 (2000).
20. Sarri G., Schumaker W., Di Piazza A., Vargas M., Dromey B., Dieckmann M.E., Chvykov V., Maksimchuk A., Yanovsky V., He Z.H., Hou B.X., Nees J.A., Thomas A.G.R., Keitel C.H., Zepf M., Krushelnick K. *Phys. Rev. Lett.*, **110**, 255002 (2013).
21. Williams G.J., Pollock B.B., Albert F., Park J., Chen Hui. *Phys. Plasmas*, **22**, 093115 (2015).
22. Sarri G., Poder K., Cole J.M., Schumaker W., Di Piazza A., Reville B., Dzelzainis T., Doria D., Gizzi L.A., Grittani G., Kar S., Keitel C.H., Krushelnick K., Kusche S., Mangles S.P.D., Najmudin Z., Shukla N., Silva L.O., Symes D., Thomas A.G.R., Vargas M., Vieira J., Zepf M. *Nat. Commun.*, **6**, 6747 (2015).
23. Xu T., Shen B., Xu J., Li S., Yu Y., Li J., Lu X., Wang C., Wang X., Liang X., Leng Y., Li R., Xu Z. *Phys. Plasmas*, **23**, 033109 (2016).
24. Ecklund S., in *Workshop on Intense Positron Beams* (Idaho Falls, USA, 1987) SLAC-PUB-4437.
25. <http://geant4.web.cern.ch/geant4/UserDocumentation/UsersGuides/PhysicsReferenceManual/fo/PhysicsReferenceManual.pdf>.
26. Ivanov K.A., Shulyapov S.A., Turinge A.A., Brantov A.V., Uryupina D.S., Volkov R.V., Rusakov A.V., Djilkibaev R.M., Nedorezov V.G., Bychenkov V.Yu., Savel'ev A.B. *Contrib. Plasm. Phys.*, **53**, 116 (2013).
27. Shulyapov S.A., Ivanov K., Tsymbalov I.N., Krestovskikh D.A., Savel'ev A.B., Ksenofontov P.A., Brantov A.V., Bychenkov V.Yu., *J. Phys. Conf. Ser.*, **653** (3), 012007 (2015).
28. Ivanov K.A., Tsymbalov I.N., Shulyapov S.A., Krestovskikh D.A., Brantov A.V., Bychenkov V.Yu., Volkov R.V., Savel'ev A.B. *Phys. Plasmas* (in press, 2017).
29. Andreev A.V., Burmistrov Yu.M., Gromov A.M., et al. *Proc. XIII Intern. Seminar EMIN 2012* (Moscow, 2013) p. 148.
30. Rusakov A.V., Ivanov K.A., Borisov N.A., Tsymbalov I.N., Gorlova D.A., Lapik A.M., Lar'kin A.S., Lisin V.P., Mordvintsev I.M., Mushkarenkov A.N., Nedorezov V.G., Polonskii A.L., Savel'ev-Trofimov A.B., Turinge A.A. *Prib. Tekh. Eksp.* (in press, 2017).